Int. J. Electrochem. Sci., 15 **(2020)** 1117 – 1127, doi: 10.20964/2020.02.21

International Journal of
ELECTROCHEMICAL
SCIENCE
www.electrochemsci.org

Effect of N_2 Flow Rate on Structure and Corrosion Resistance of AlCrN Coatings Prepared by Multi-Arc Ion Plating

Ziyu Gong[1], *Rongfa Chen*[1,*], *Jing Li*[1], *Pei Cao*[1], *Haoran Geng*[1]

School of Mechanical Engineering, Yangzhou University, Yangzhou 225127, China
[*]E-mail: rfchen@yzu.edu.cn

Received: 6 October 2019 / *Accepted:* 18 November 2019 / *Published:* 31 December 2019

AlCrN coatings are deposited on high-speed steel by a multi-arc ion plating technique at various N_2 flow rates. The effects of N_2 flow rate on microstructure, elemental composition, deposition rate and corrosion properties of the AlCrN coatings are investigated. The results indicate that the macroparticles and pits on the coating surfaces can be reduced with raising the N_2 flow rate, so that the surfaces become flatter. For the N_2 flow rate ranging from 300 to 500 sccm, the phases of the coatings are composed of intermetallic phase AlN and fcc-(Cr, Al) N with (111) preferred orientation, causing the decrease of growing tendency towards preferential orientation. Then with increasing the N_2 flow rate to 700-900 sccm, the coatings exhibit a single (fcc) phase. In the case of 900 sccm, the corrosion resistance of AlCrN coated sample exhibits a improvement with the highest electrode potential and the lowest corrosion current density when compared with the other coated samples.After appropriately increasing the N_2 flow rate, the AlCrN coating becomes a potential material for corrosion resistance.

Keywords: Corrosion resistance； AlCrN； Nitrogen flow rate； Multi-arc ion plating

1. INTRODUCTION

Transition metal nitride coatings exhibit excellent tribological properties, thermal stability and relatively low residual stress, so in recent years, cemented carbide coatings and their composite coatings have attracted widespread attention [1-5]. Compared with binary nitride coatings such as CrN and TiN, AlCrN ternary nitride coatings exhibit better oxidation resistance, wear resistance, high melting point and good hardness, which is due to refinement of grain sizes caused by adding Al element [6]. Nowadays, most of the coatings with compact face-centered cubic (fcc) and smooth surfaces for good corrosion resistance are deposited by physical vapor deposition (PVD) [7,8]. Multi-arc ion plating (MAIP) technique is a common technology for the deposition of AlCrN coatings. Among all kinds of PVD techniques, MAIP has been widely applied to industrial production due to its high deposition rate and excellent interface bonding strength between coatings and substrates [9]. In order to improve the

properties of AlCrN coatings, many scholars have done a lot of researches. For example: (1) deposition of multilayer coatings to enhance the properties of the coatings, such as AlCrN/Cr/AlCrN [10], AlCrN/TiAlSiN [11], etc; (2) adjust the application environment of the coatings, such as dry, wet and cryogenic conditions [12]; (3) heat treatment of the substrates [13]. But unfortunately, in actual practice, due to the rapid deposition rate, local defects often occur on the coating surfaces, these inevitable local defects usually exist in the form of macroparticles and pits [14]. These macroparticles affect the corrosion resistance of the coatings to a certain extent. In addition, when the electrochemical potential difference exists between the substrate surface and the coating surface, a severe electrochemical corrosion will occur [15]. Therefore, optimizing the parameters of multi-arc ion plating technique is of great significance to improve the corrosion resistance of AlCrN coatings. Moreover, studies have shown that nitrides have a great influence on the structure and properties of the coatings [16]. During the deposition process of the coatings, the appropriate adjustment of N_2 flow rate may affect the nucleation and growth kinetics of the coatings, and finally change microstructure and performance of the coatings [10]. At present, studies have been conducted to improve the bonding strength between AlCrN coating and substrate by adjusting the deposition parameters such as substrate bias voltage and nitrogen partial pressure [6]. But currently, few studies focus on the effect of deposition parameters on the corrosion resistance of AlCrN coating.

In this study, the AlCrN coatings were prepared by MAIP on high-speed steel substrates by varying N_2 flow rate. The effects of N_2 flow rate on the morphology, deposition rate, composition, phase composition and the anti-corrosion property of the AlCrN coatings were investigated.

2. EXPERIMENT

2.1 Sample preparation

In this study, high-speed steel with the dimension of Φ40×5 mm was used as the substrate, and the substrate surface was polished to achieve a mirror effect where the roughness value was less than 0.02 mm. Then the substrate was sandblasted using a sandblasting machine(SJK-9070) to increase the coating-substrate adhesion, so as to improve the durability of the coating. After sandblasting, the substrate was cleaned for 40 min by a ultrasonic cleaning instrument (XL-A090168).

AlCrN coatings were deposited in a multi-arc ion plating reactor (Fig. 1), the targets of Cr and Al prepared by hot isostatic pressing are equipped on the same side of the reactor chamber, both of them are in the diameter of 100 mm and purity of 99.99%. The coatings were deposited at a stable temperature between 450 ℃ and 500 ℃. Before deposition, the substrate was cleaned by Ar_2 glow discharge plasma at the bias voltage of -700 V for 2 min with the duty cycle of 60%. The N_2 flow rate was tuned at 300, 500, 700 or 900 sccm, while the Ar_2 flow rate was varied at 900, 700, 500, or 300 sccm respectively to keep the chamber pressure at 5.5×10^{-3} Pa for tracking the properties of coatings as a function of N_2 flow rate. Meanwhile other parameters remained unchanged. The deposition time was around 50 min, and the bias voltage was set at -65 V,

2.2. Coating characterization

The surface and cross-sectional morphologies of the coatings were characterized by a Field Emission Scanning Electron Microscope (FE-SEM, Gemini 300) system operated at 15 kV with an energy dispersive spectrometer (EDS) at 20 kV. The crystal analysis of the AlCrN coatings was conducted by an x-ray diffractometer (XRD, D8 Advance, Bruker, Germany) with Cu-K α radiation, which was operated with a step by step scanning length of 0.5° . The 2 θ range was 20-90° with a scanning rate of 5°/min.

Electrochemical potentiodynamic polarization tests of the AlCrN coatings were operated by a electrochemical workstation(CHI660E). The potentiodynamic polarization curves (E/I) were measured in a three-electrode cell with a platinum slice as a counter electrode, and a saturated calomel electrode (SCE) was selected as a reference electrode. The experiments were carried out in 3.5 wt% NaCl corrosion solution at room temperature, the effective area of the samples was approximately 1 cm^2, and they were immersed in 3.5 wt% NaCl corrosion solution for 20 minutes before testing. All the potentiodynamic polarization studies were conducted after stabilization of the open circuit potential (OCP). The scan rate used for polarization curves was fixed at 1.5 mV/s.

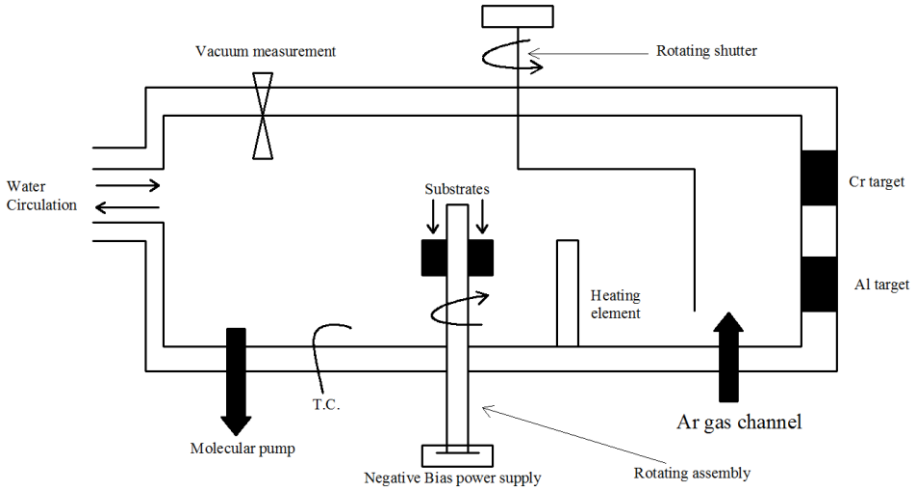

Figure 1. Schematic diagram of the multi-arc ion plating system.

3. RESULTS AND DISCUSSION

3.1 Deposition rate

The evolution of deposition rate with N_2 flow rate is shown in Fig. 2. It is found that with the N_2 flow rate increasing from 300 to 700 sccm, the deposition rate was obviously decreased from 0.67 to 0.47 nm/min. However, the deposition rate seems not to be changed when the N2 flow rate was further increased from 700 to 900 sccm. When the N_2 flow rate was increased from 300 to 700 sccm, the significant decline of deposition rate may be due to the sputtering ability of nitrogen is lower than that of argon [17], which leads to a decrease of sputtering yield on target surface, so the deposition rate was

reduced. Until the N_2 flow rate reached 700 sccm, the deposition rate tended to be stable, it can be explained by the "target poisoning" [18,19]. The process can be expressed as [10]:

$$Al^{3+} + Cr^{3+} \xrightarrow{N_2(300-700sccm)} AlCrN \quad (1)$$

$$\mathrm{AlCrN} \xrightarrow{N_2(700-900sccm)} AlCrN \quad (2)$$

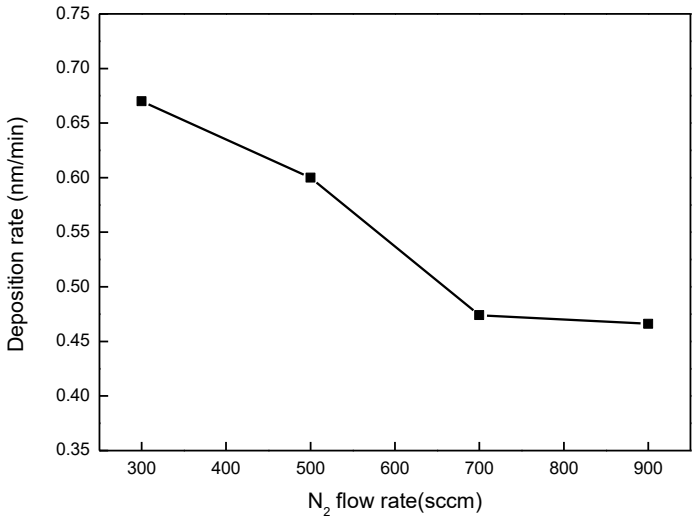

Figure 2. Evolution of deposition rate of the AlCrN coatings with the N_2 flow rate from 300 to 900 sccm.

3.2 Phase structure analysis

Fig 3 shows the X-ray diffraction patterns of the AlCrN coatings prepared at various N_2 flow rates. Generally, two phases which are the fcc structure related to (Cr, Al)N and the intermetallic structure related to AlN can be seen in the patterns [20]. Moreover, the peak presents at 30.17° which is corresponding to the (100) plane of AlN, and the peaks at 2θ=37.6° , 44.63° and 76.99° are related to the (111), (200) and (220) planes of (Cr, Al)N. In the N_2 flow rate range from 300 to 500 sccm, both of the AlN and (Cr, Al)N crystals can be identified in the coatings. With raising the N_2 flow rate to 700 sccm, the AlN peak disappeared and the intensity of the (Cr, Al)N peaks slightly decreased, which were further reduced in the case of 900 sccm.This phenomenon can be explained that in the range of 300-500 sccm, Al atoms are more than Cr atoms. Al replaced Cr which was separated from CrN, when the replacement reached a certain limit, AlN was produced by the reaction of Al atoms with nitrogen [21]. With increasing the N_2 flow rate, Al content decreased and replacement failed to reach the limit, which caused the decrease of the AlN (100) peak. In addition, the intensity of the (Cr, Al)N (111) diffraction peak decreased significantly with the increase of the N_2 flow rate at 900 sccm. At the same time, (Cr, Al)N (111) diffraction peak shifted slightly to lower 2 θ angles. This result indicates that the substitution solid solution was formed when Cr was replaced by Al. Smaller Al atoms occupied some Cr sites to form the solid solution [10], causing a decline in the lattice parameters, the grain size of the AlCrN coatings were calculated from the X-ray diffraction and found to decrease with increasing N_2 flow rate, which can be explained by the mobility of atoms in deposited AlCrN coatings as a result of the increase in Al/Cr ratio [22].

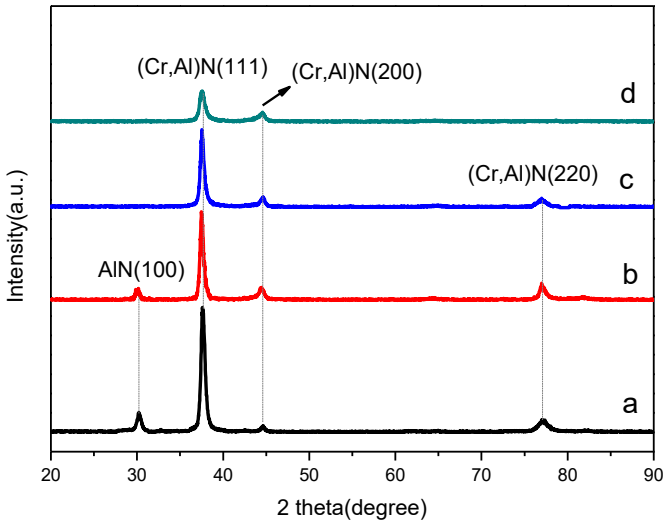

Figure 3. XRD patterns of the the AlCrN coatings, deposited at the N_2 flow rate of (a) 300 sccm; (b) 500 sccm; (c) 700 sccm; (d) 900 sccm with a scanning rate of 5°/min and a step by step scanning length of 0.5°

3.3 Morphology observation

3.3.1 Surface topography and composition analysis

The surface morphologies of the AlCrN coatings are shown in Fig. 4. It is found that macroparticles and pits are distributed on the surfaces of the AlCrN coatings. When the N_2 flow rate was 300 sccm, the macroparticles on the coating surface were obviously peeling off, showing large-sized pits. With the N_2 flow rate going up to 500-700 sccm, no significant peelings of macroparticles can be observed, and the size of the macroparticles was significantly reduced. As the N_2 flow rate reached 900 sccm, the coating surface became flatter and more uniform. During the deposition process, arcs discharged on the target surface and produced macroparticles which could be splattered onto the coating surface [23]. These macroparticles peeled off during the sputtering process, resulting pits [24]. With N_2 flow rate increasing gradually, more N^+ accumulated on the Al and Cr target surface, producing more nitrides. Due to the combination of nitrides with Al and Cr, the nitrides may be difficult to sputter from the target surface. Thus the sputtering degree decreased, and the existing particles were splashed. Hence, the probability of the subsequent particles depositing on the existing macroparticles to cover them decreased, prolonging the diffusion time of macroparticles, leading to a drop in the number of macroparticles, thus a relatively flat coating surface can be obtained by properly increasing N_2 flow rate [25].

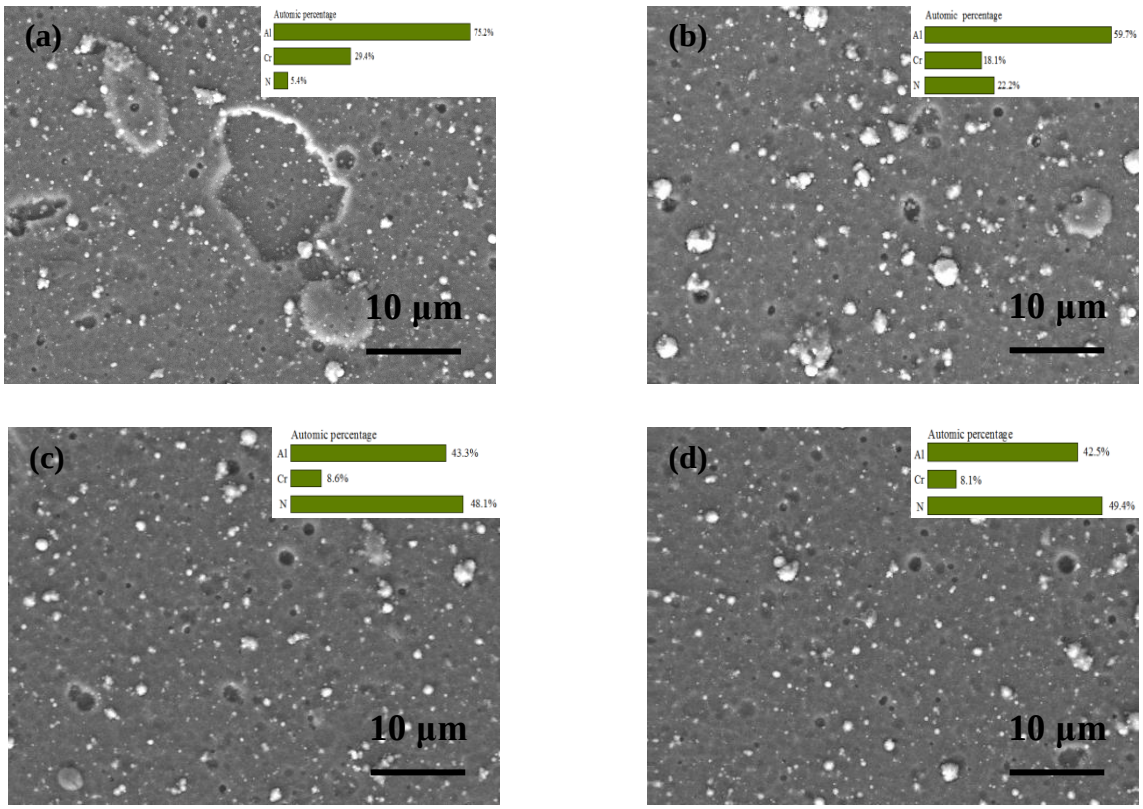

Figure 4. Surface FE-SEM morphologies of the AlCrN coatings, deposited at the N_2 flow rate of (a) 300 sccm; (b) 500 sccm; (c) 700 sccm; (d) 900 sccm

The results of the elemental composition are shown in Table 1. With increasing the N_2 flow rate, the content of Cr and Al decreased, and the content of N_2 increased accordingly. Meanwhile, the increase in the ratio of Al/Cr can be explained by the sputtering threshold energy of Al (13 eV) is lower than that of Cr (22 eV) [26]. When the N_2 flow rate reached 700 sccm, the phenomenon of "target poisoning" occurred as a result of the stable Al/Cr and (Al+Cr)/N ratios. It can be explained by the difference between the sputtering yield and degree of ionization when the AlCrN layer formed on the target surface [10].

Table 1. Elemental composition analysis of AlCrN coatings deposited at different N_2 flow rates

N_2 flow rate / sccm	Al/%	Cr/%	N/%	Al/Cr	N/(Al+Cr)
300	75.2	29.4	5.4	2.56	0.05
500	59.7	18.1	22.2	3.30	0.29
700	43.3	8.6	48.1	5.03	0.93
900	42.5	8.1	49.4	5.25	0.98

3.3.2 Cross-section Morphology

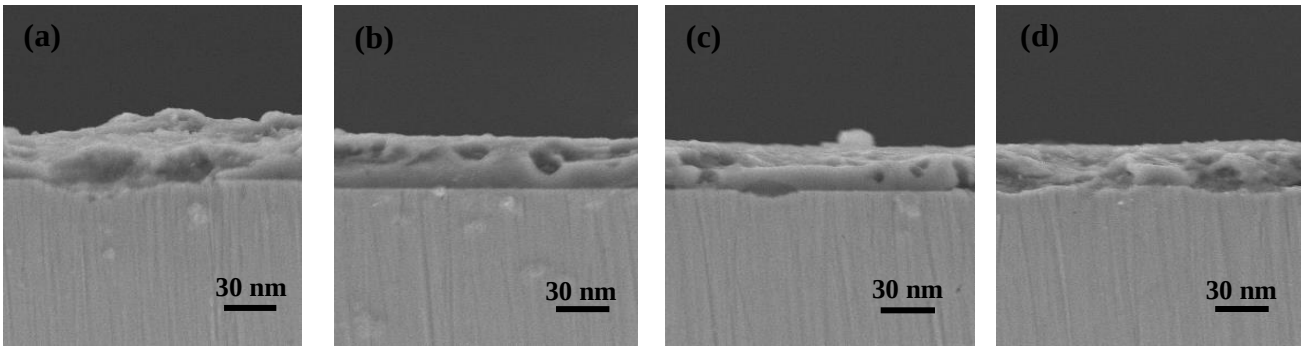

Figure 5. Cross-sectional FE-SEM images of the AlCrN coatings, deposited at the N_2 flow rate of (a) 300 sccm; (b) 500 sccm; (c) 700 sccm; (d) 900 sccm.

The cross-sectional morphologies of the AlCrN coatings are presented in Fig. 5. It can be measured that the coating thicknesses with the N_2 flow rate of 300, 500, 700 and 900 sccm are 33.3 nm, 30 nm, 23.7 nm and 23.3 nm, it is reduced continuously. Because the "target poisoning" reduced the deposition rate, which led to a thinner but uniform coating.

3.5 Corrosion behavior

The polarization curves dealt with Gamry Echem Analyst software are shown in Fig. 6. The corrosion current density (I_{corr}) and corrosion potential (E_{corr}) were obtained from the Tafel extrapolation method, as listed in Table 2. When the N_2 flow rate was increased from 300 to 900 sccm, the corrosion current density was decreased from 20.31 $\mu A \cdot cm^{-2}$ to 0.42 $\mu A \cdot cm^{-2}$, while the corrosion potential was improved from -0.508V for 300 sccm to -0.367V for 900 sccm.

The corrosion performance of the coatings is usually related to its corrosion current density and corrosion potential. The corrosion current density can be used to characterize the degree of corrosion on the coating surfaces [27]. It is a key parameter for evaluating the corrosion resistance of the coatings. The smaller values of the corrosion current density represent higher corrosion resistance [28]. The electrode potential is a thermodynamic parameter that reflects the tendency of the material to corrode [29]. The positive shift of the corrosion potential with increasing N_2 flow rate represents a noble electrode potential resistance being attained, which indicates the improvement of corrosion resistance of the AlCrN coatings [15]. Hence, the sample coated by higher N_2 flow rate has better corrosion resistance than those of lower N_2 flow rate.

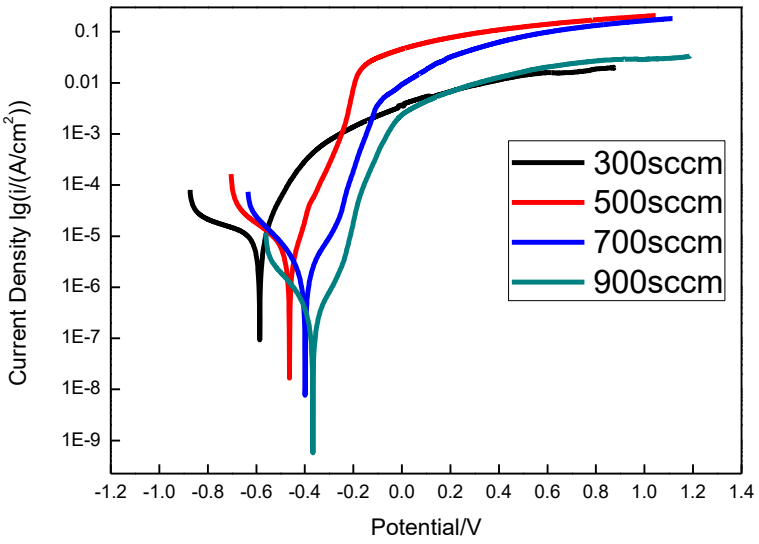

Figure 6. Potentiodynamic polarization curves of the AlCrN coatings corroded in 3.5wt% NaCl solution. Scan rate: 1.5 mV/s.

Table 2. Results of polarization curves of the AlCrN coatings corroded in 3.5 wt% NaCl solution.

N_2 flow rate / sccm	I_{corr} / μA·cm^{-2}	E_{corr} / V
300	20.31	-0.508
500	5.37	-0.463
700	1.42	-0.399
900	0.42	-0.367

Fig. 7 shows the corroded surface morphologies of the AlCrN coatings after polarization reactions. In the case of the N_2 flow rate of 300 sccm, there are obvious corrosion pores appeared on the coating surface owing to the existence of some macroparticles and pits, and some macroparticles peeled off because of the attacks by electrode and current [30]. With the N_2 flow rate increased to 900 sccm, the coating surface after corrosion tests exhibits no obvious corrosion pores. For the as-deposited AlCrN samples, although transition metal nitride coatings have a protective effect on the surface against corrosive environments [31], the columnar structure of AlCrN appears to encourage the formation of defects on the surface [32]. As the N_2 flow rate increased, more nitrogen atoms combined with Al and Cr ions to form more nitrides. These nitrides formed a solid dense barrier between the coatings and the NaCl, protecting the underlying alloy from dissolution. This is because the corrosion product is insoluble in NaCl solution and acts as a barrier to the corrosive environment [33]. This hindrance caused a delay in the dissolution process and consequently reduced the corrosion rate. The experimental phenomenon indicates that the corrosion resistance of the material is closely related to the microstructure. The fewer defects and the higher density, the better the corrosion resistance of the coatings. This can be explained by that the formation of dense and compact microstructure reduced the permeation of corrosive media

through macroparticles and pits [34]. According to the results of XRD, grain refinement means an increase in grain boundary density, which can form a homogenous and dense passive film to obtain a better corrosion resistance [35].

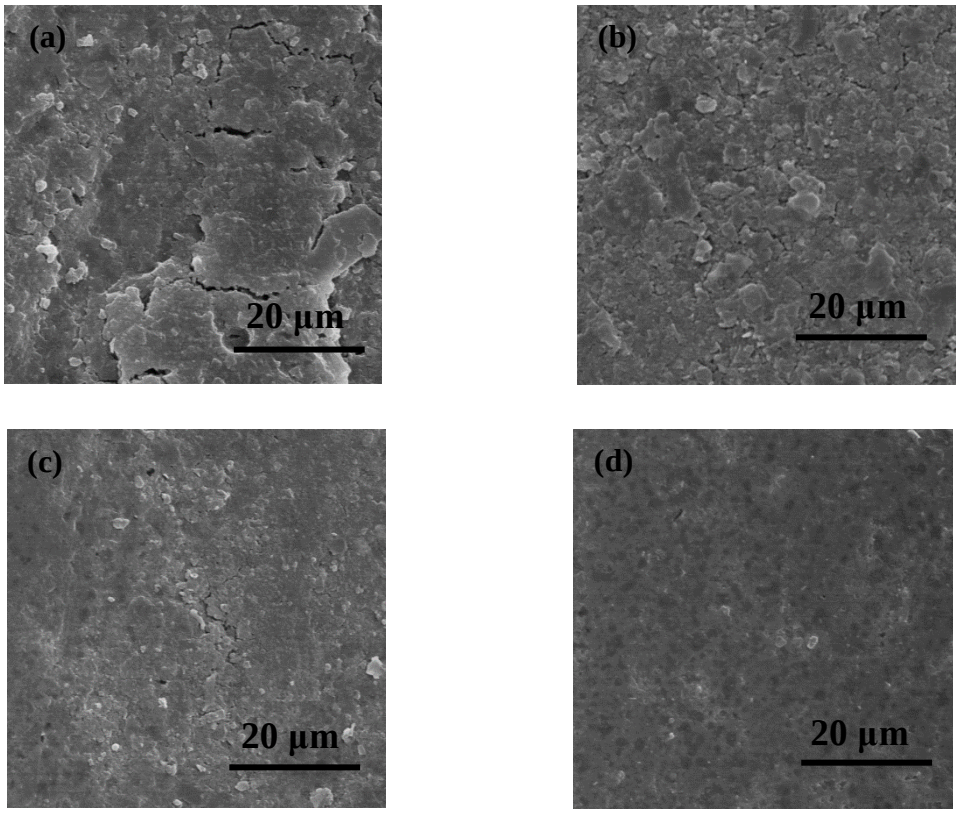

Figure 7. The corroded surface morphologies of the AlCrN coatings after polarization reactions in 3.5% NaCl solution: (a) 300 sccm; (b) 500 sccm; (c) 700 sccm; (d) 900 sccm

4. CONCLUSION

Potentiodynamic polarization experiment was used to study the effects of N_2 flow rate on the corrosion behavior of AlCrN coatings prepared by the multi-arc ion plating technique. While the deposition rate, phase transformation and microstructure of the as-deposited samples were analyzed. It is found that the deposition rate was reduced with increasing N_2 flow rate from 300 to 700 sccm, and the coating crystallization was in fcc and intermetallic phase structure. Then the deposition rate became stable in the range of 700-900 sccm since the target surface appeared "target poisoning phenomenon", while the coating phase was changed to a fcc single phase structure. The grain size of the AlCrN coatings presented a down trend with increasing N_2 flow rate, and the number of macroparticles and pits reduced and the coating surface became flatter. Results of potentiodynamic polarization curves shown that the specimen coated by higher N_2 flow rate has better corrosion resistance than those of lower N_2 flow rate.

The formation of dense and compact microstructure and grain refinement by increasing N_2 flow rate can improve the corrosion resistance of the AlCrN coatings in 3.5 wt% NaCl corrosion solution.

ACKNOWLEDGEMENTS
This research was financially supported by the Municipal University Cooperation Fund Project of Yangzhou (No. YZ2017294 and No. YZ2019129).

References

1. J. Zhang, Q. Xue, S. Li, *Appl. Surf. Sci.*, 280 (2013) 626.
2. X. Zhang, X. Tian, Z. Zhao, J. Gao, Y. Zhou, P. Gao, Y. Guo, Z. Lv, *Surf.Coat.Technol.,*364 (2019) 135.
3. B. Gao, X. Du, Y. Li, S. Wei, X. Zhu, Z. Song, *J. Alloys Compd.,* 797 (2019) 1.
4. S. Wan, H. Wang, Y. Xia, A. Tieu, B. Tran, H. Zhu, G. Zhang, Q. Zhu, *wear*, 432-433 (2019) 202940.
5. S. Zhou, L. Wang, Q. Xue, *Surf. Coat. Tech.*, 206 (2011) 387.
6. L. Wang, S. Zhang, Z. Chen, J. Li, M. Li, *Appl. Surf. Sci.,* 258 (2012) 3629.
7. M. Chen, D. Wu, W. Chen, S. Zhang, *Thin Solid Films,* 612 (2016) 400.
8. Z. Lei, Q. Zhang, X. Zhu, D. Ma, F. Ma, Z. Song, Y. Fu, *Appl. Surf. Sci*., 431 (2018) 170.
9. K. Jiang, D. Zhao, X. Jiang, Q. Huang, L. Miao, H. Lu, Y. Li, *J. Alloys Compd.,* 750 (2018) 560.
10. Q. Li, X. Cheng, D. Gong, W. Ye, *Thin Solid Films,* 675 (2019) 74.
11. B. Xiao, J. Liu, F. Liu, X. Zhong, X. Xiao, T. Zhang, Q. Wang, *Ceram. Int.,* 44 (2018) 23150.
12. V. Varghese, Akhil K., M. Ramesh, D. Chakradhar, *J. Manuf Process.,* 43 (2019) 136.
13. W. Chen, J. Zheng, X. Meng, S. Kwon, S. Zhang, *Vacuum,* 121 (2015) 194.
14. A. Ruden, E. Restrepo-Parra, A.U.Paladines, F. Sequeda, *Appl. Surf. Sci.,* 270 (2013) 150.
15. D. Wang, M. Hu, D. Jiang, Y. Fu, Q. Wang, J. Yang, J. Sun, L. Weng, *Vacuum,* 143 (2017) 329.
16. L. Shan, Y. Wang, J. Li, J. Chen, *Surf. Coat. Tech.,* 242 (2014) 74.
17. G. Zhang, P. Yan, P. Wang, Y. Chen, J. Zhang, *Mater. Sci. Eng: A.,* 460-461 (2007) 301.
18. M. Arif, C. Eisenmenger-Sittner, *Surf. Coat. Tech.*, 324 (2017) 345.
19. J. Posada, A. Bousquet, M. Jubault, D. Lincot, E. Tomasella, *Plasma. Process. Polym.,* 13 (2016) 997.
20. H. Chen, Y. Chan, J. Lee, J. Duh, *Surf. Coat. Tech.,* 205 (2010) 1189.
21. M. Zhou, Y. Makion, M. Nose, K. Nogi, *Thin Solid Films,* 339 (1999) 203.
22. A. Inoue, T. Zhang, T. Masumotoa, *J. Non-cryst Solids.,* 156-158 (1993) 473.
23. R. Boxman, S. Goldsmith, *Surf. Coat. Tech.,* 52 (1992) 39.
24. X. Guan, Y. Wang, G. Zhang, X. Jiang, L. Wang, Q. Xue, *Tribol. Int.,* 106 (2017) 78.
25. M. Aguas, A. Nartowski, I. Parkin, *J. Mater Chem,* 8 (1998) 1875.
26. K. Wasa, M. Kitabatake, H. Adachi, *Thin Film Materials Technology: Sputtering of Compound Materials.* William Andrew Publishing, (2004) Norwich, USA.
27. Wilcox, G. D., Gabe, D.R., Faraday's Laws of Electrolysis, *Transactions of the Imf,* 70 (1992) 93.
28. W. Ye, Y. Li, F. H. Wang, *Electrochim. Acta.,* 54 (2009) 1339.
29. M. Yamashita, H. Nagano, R.A. Oriani, *Corros. Sci*., 40 (1998) 1447.
30. G. Li, L. Zhang, F. Cai, Y. Yang, Q. Wang, S. Zhang, *Surf. Coat. Tech.,* 366 (2019) 355.
31. S. Abusuilik, K. Inoue, *Surf.Coat.Tech.,* 237 (2013) 421.
32. A. Yetim, A. Alsaran, A. Celik, *Corros. Eng. Sci. Techn.,* 46 (2011) 439.
33. L. Liu, Y. Li, F. Wang, *J. Mater. Sci.,* 26 (2010) 1.

34. Y. Liu, X. Wang, J. Luo, X. Lu, *Appl. Surf. Sci.,* 225 (2009) 9430.
35. X. Wei, D. Zhu, X. Ling, L. Yu, M. Dai, *Int. J. Electrochem. Sci.,* 13 (2018) 4198.